Calculation of Helicon Propagation and Gantmakher-Kaner Oscillations in Copper*

L. T. Wood and S. D. Yesavage
Department of Physics, University of Houston, Houston, Texas 77004
(Received 14 February 1972)

The transmission of electromagnetic fields through thin copper slabs with the magnetic field $\vec{B}_0$ and the propagation vector $\vec{q}$ along the [001] and [111] directions has been investigated numerically and the results compared with experimental results of Wood and Gavenda. The conductivity tensor used in the calculations is derived from a model Fermi surface proposed by Halse. Only the variation of the area A enclosed by the charge carriers and the derivatives of the area with respect to k_z, $\partial A/\partial k_z$ are considered. For $\vec{B}_0 \parallel [001]$, the calculated and experimental values of the helicon edge differ less than 3% for the frequencies studied. The electrons responsible for the helicon edge are associated with a value 9.5×10^8 cm^{-1} for $|\partial A/\partial k_z|$. A discussion of the relative damping effects by the charge carriers is given. For $\vec{B}_0 \parallel [111]$, Gantmakher-Kaner (GK) oscillations with a period of 590 G are observed in both the calculated and experimental results. The amplitude modulation of the GK oscillations leads to an interpretation in terms of a beating of two separate sets of GK oscillations, one set associated with a maximum in $|\partial A/\partial k_z|$ and the other set associated with a minimum in $|\partial A/\partial k_z|$.

I. INTRODUCTION

Recently, there have been several papers[1-3] which develop the theory of the transmission of electromagnetic fields through metal slabs in the presence of a magnetic field normal to the sample surface. The boundary conditions on the electromagnetic fields have been explicitly included in these developments, and the transmission spectrum of the electromagnetic fields has been calculated for several model Fermi surfaces.[3] The results from these model-Fermi-surface calculations have compared qualitatively quite well with experimental results.[4] These model-Fermi-surface calculations, however, suffer from the disadvantage that quantitative comparison with experimental results is not very practical. In this paper we present calculated results for the transmission of electromagnetic fields through single crystals of copper with the magnetic field parallel to the [001] and [111] axes. These calculated results are compared with the previous experimental results of Wood and Gavenda.[5] The electromagnetic fields under consideration are the helicon waves[6-9] and the Gantmakher-Kaner (GK) oscillations.[10]

In Sec. II the theoretical ideas are reviewed, in Sec. III the techniques of computation are presented, and in Sec. IV the results and their interpretation are given.

II. THEORY

The infinite-medium dispersion relation for a helicon wave propagating along a static magnetic field $\vec{B}_0$ (taken to be along the z axis) is given by

$$q_\pm^2 = (4\pi\omega/ic^2)\sigma_\pm(q, \omega, B_0) , \tag{1}$$

where q is the complex wave number, ω is the angular frequency, $\sigma_\pm = \sigma_{xx} \mp i\sigma_{xy}$ is the conductivity for the left- and right-circularly polarized waves, and c is the speed of light. In general, the components of the conductivity tensor $\sigma_{\alpha\beta}(\alpha, \beta \rightarrow x, y, z)$ must be calculated by solving the Boltzmann transport equation. The result of such a calculation has been found by Mertsching[11] to be

$$\sigma_{\alpha\beta} = \frac{2e^2}{h^2}\int_{-k_z^{\max}}^{+k_z^{\max}} m_c\, dk_z \sum_{n=-\infty}^{\infty} \frac{v_{n\alpha} v_{n\beta}^*}{1/\tau + i(\vec{q}\cdot\vec{v}_z - \omega - n\omega_c)} , \tag{2}$$

where

$$v_{n\alpha} = \frac{\omega_c}{2\pi}\int_0^{2\pi/\omega_c} dt\, v_\alpha(t) \times \exp\left(-i\int_0^t dt' \,(\vec{q}\cdot[\vec{v}(t') - \bar{v}_z\hat{z}] + n\omega_c)\right) . \tag{3}$$

Here ω_c is the cyclotron frequency, m_c is the cyclotron mass, and τ is the relaxation time of the charge carriers. For a Fermi surface which has cylindrical symmetry about the magnetic field, the conductivity calculated from Eq. (2) is found to be[12,13]

$$\sigma_\pm = \frac{iec}{4\pi^3 B_0}\int_{-k_z^{\max}}^{+k_z^{\max}} \frac{A(k_z)dk}{(\pm 1 - x) + i\epsilon} , \tag{4}$$

where $\epsilon = (\omega_c\tau)^{-1}$ and

$$x = (hc\,q/2\pi eB_0)(\partial A/\partial k_z) = qv_z/\omega_c . \tag{5}$$

$A(k_z)$ is the cross-sectional area enclosed by a charge carrier as it executes an orbit on the k_z = const planes, and v_z is the z component of the carrier velocity.

If a metallic slab (lying between $z = 0$ and $z = L$) extends to infinity in the x and y directions and if one assumes specular reflection of the electrons at

the boundaries of the slab, then the electromagnetic field may be calculated by repeating the slab to infinity in both positive- and negative-z directions and forcing the electric field and its derivatives to assume given values at the "boundaries" of the slabs.[1,3] For circularly polarized waves incident on a metallic slab, the ratio of the transmitted electric field to the incident electric field $E_{\pm t}/E_{\pm i}$ is given by[3]

$$\frac{E_{\pm t}}{E_{\pm i}} = -\frac{2iqA_{\pm}(L)}{q^2B_{\pm}^2(L) - q^2A_{\pm}^2(L) + 1} , \tag{6}$$

where q is the free-space wave number and $A_{\pm}(L)$ and $B_{\pm}(L)$ are given by

$$A_{\pm}(L) = -\frac{1}{L}\sum_{n=0}^{\infty}\frac{(2-\delta_{n0})\cos(q_nL)}{q_n^2 - q^2[K + (4\pi/i\omega)\sigma_{\pm}(q_n)]} \tag{7}$$

and

$$B_{\pm}(L) = -\frac{1}{L}\sum_{n=0}^{\infty}\frac{(2-\delta_{n0})(-1)^n\cos(q_nL)}{q_n^2 - q^2[K + (4\pi/i\omega)\sigma_{\pm}(q_n)]} . \tag{8}$$

Equation (6) has been corrected for a sign error and an exponent error. Here $q_n = n\pi/L$, and K is the ionic dielectric constant. For frequencies of interest here the displacement current can be neglected (this means K is neglected), and the dependence of σ on ω can also be neglected. Furthermore, the quantities $q^2B_{\pm}^2(L)$ and $q^2A_{\pm}^2(L)$ are both very small compared to 1 (this has been verified numerically over the entire range of magnetic fields and frequencies used in the experiments) so the information about $E_{\pm t}/E_{\pm i}$ is contained in $A_{\pm}(L)$. The principal contribution to the sum occurs when the denominator in Eq. (7) vanishes. The denominator vanishes whenever the helicon dispersion relation is satisfied. The helicon then propagates whenever q is essentially real ($\mathrm{Re}\sigma_{\pm} \ll \mathrm{Im}\sigma_{\pm}$) and will be damped if q has an appreciable imaginary part ($\mathrm{Re}\sigma_{\pm} \approx \mathrm{Im}\sigma_{\pm}$). It has also been shown[3,10,14] that GK oscillations occur whenever the condition $\omega_c = qv_z$ is satisfied. This is just the condition for Doppler-shifted cyclotron resonance[15] (DSCR) of an electron drifting along the z direction with velocity v_z. The period ΔB_0 of these GK oscillations is given by

$$\Delta B_0 = (hc/eL)\left|\partial A/\partial k_z\right|_{\mathrm{ext}} . \tag{9}$$

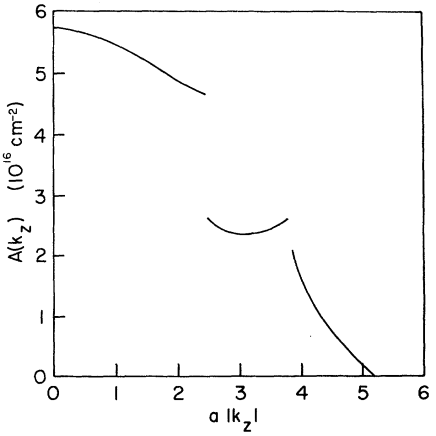

FIG. 1. Area vs $a|k_z|$ for copper Fermi surface with k_z along [001]. a is the lattice constant. The section extending from $a|k_z| = 2.50$ to $a|k_z| = 3.80$ consists of the four-cornered-rosette hole orbits.

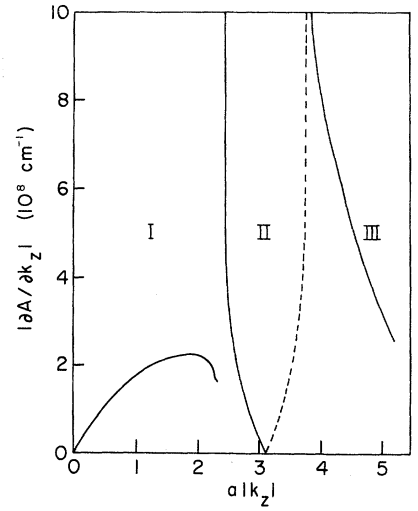

FIG. 2. $|\partial A/\partial k_z|$ vs $a|k_z|$ for copper Fermi surface with k_z along [001]. The dashed line indicates where $\partial A/\partial k_z$ is positive, the solid where it is negative.

III. TECHNIQUES OF CALCULATION

Copper was chosen for this investigation because it has a nontrivial yet well-known Fermi surface and because a number of experiments[4,5,16-18] on helicon propagation and GK oscillations were available for comparison. Furthermore, when the magnetic field is parallel to the [001] or [111] axis, no open orbits exist, and calculation of the conductivity is straightforward. In this calculation the Fermi surface of copper is treated as cylindrically symmetric; i. e., only the areas and derivatives of the areas with respect to k_z enter the calculation. The area and derivatives of the areas are calculated from the parameters given by Halse.[19] $A(k_z)$ and $\partial A/\partial k_z$ were calculated for increments of $\Delta Z = 0.05$, where ΔZ is a dimensionless parameter given by $\Delta Z = a\Delta k_z$, and a is the lattice constant. This is equivalent to using two hundred twelve bands to cover the entire Fermi surface in the [001] direction and two hundred twenty bands for the [111] direction. The variation of $A(k_z)$ and $\partial A/\partial k_z$ with $\vec{B}_0 \| [001]$ and $\vec{B}_0 \| [111]$ is shown in Figs. 1-4. A standard Simpson's one third rule was used for the numerical integration for the conductivity.

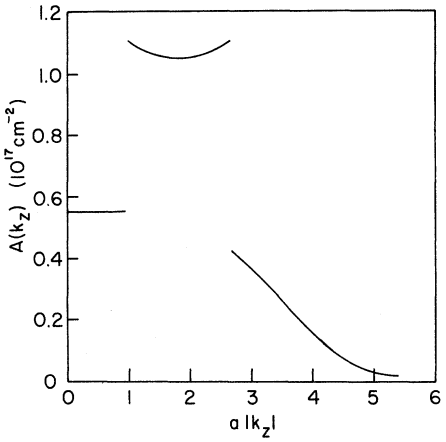

FIG. 3. Area vs $a|k_z|$ for copper Fermi surface with k_z along [111]. The section extending from $a|k_z| = 1.00$ to $a|k_z| = 2.65$ consists of the six-cornered-rosette hole orbits.

In evaluating the infinite sums some criterion must be established for terminating the sums. For the local regime ($ql \ll 1$), where the helicon is propagating, a few terms give very good convergence. For the nonlocal regime ($ql \geq 1$), however, one must include more terms in the sum. The sums calculated here were terminated when the error produced by 50 succeeding terms caused a change of less than 0.5% in the principal sum. This criterion was satisfied when about 200 terms were included in the sums. As a check, the transmitted electric fields were calculated for a spherical Fermi surface, once using the analytic expression[20] for the conductivity and once using the numerical evaluation of the conductivity. The results differed by less than 0.5%.

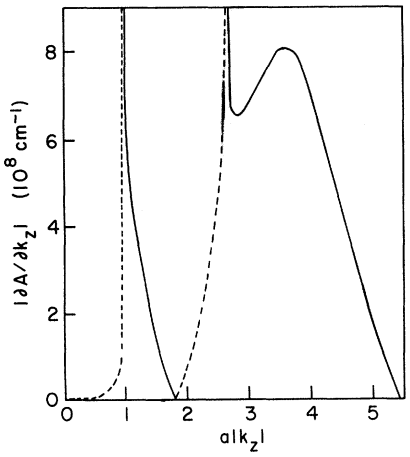

FIG. 4. $|\partial A/\partial k_z|$ vs $a|k_z|$ for copper Fermi surface with k_z along [111]. The dashed line indicates where $\partial A/\partial k_z$ is positive, the solid where it is negative.

The variation in the cyclotron mass was calculated assuming the Halse Fermi surface to be valid for energies near the Fermi energy. This is equivalent to assuming the velocity of an electron is directly proportional to the gradient of the Fermi surface. For the [001] and [111] axes this assumption gives good agreement with the measured cyclotron masses.[21,22]

IV. NUMERICAL RESULTS AND INTERPRETATION

A. Results and Interpretation for $\vec{B}_0 \parallel [001]$

In Fig. 5, we show (a) the experimental and (b) the calculated curves for the transmitted signal versus $\vec{B}_0$ for $\vec{B}_0 \parallel [001]$. The experimental curve is the result of beating a reference signal with the signal picked up by a receiving coil.[5] The calculated curve is the real part of the ratio of the transmitted electric field to the incident electric field [this quantity is designated as $\mathrm{Re}(E_t/E_i)$]. The amplitude of the calculated curve has been normalized with respect to the experimental curve for an arbitrary B_0. No GK oscillations are observed in either curve, but the helicon edge (the minimum magnetic field at which the helicon propagates) in the calculated curve is in good agreement with that in the experimental curve. In Table I, we show the helicon edge for several frequencies investigated. Since the helicon edges are not very sharp, the relaxation time was increased to 10^{-9} sec in the determination of the helicon edge in the

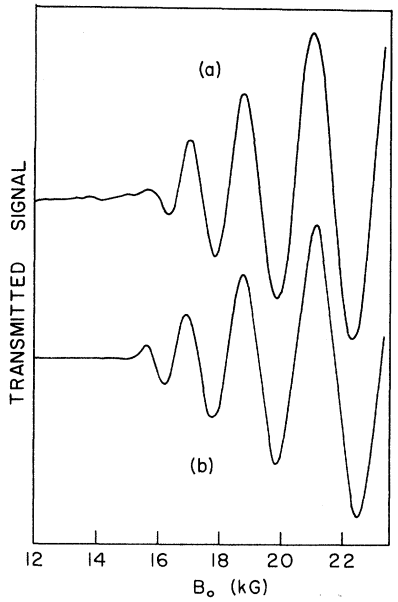

FIG. 5. (a) Experimental transmitted signal versus B_0 for $\vec{B}_0 \parallel [001]$ with $f = 395.26$ kHz. (b) Calculated transmitted signal versus B_0 for $\vec{B}_0 \parallel [001]$ with $f = 395.26$ kHz and $\tau = 10^{-10}$ sec. The specimen thickness is 0.84 mm for each curve.

TABLE I. Helicon edge as a function of frequency.

Frequency (kHz)	Helicon edge (kG) Experimental value	Calculated value
395.26	15.3	15.1
200.00	12.2	12.1
599.97	17.8	17.4
800.00	19.5	19.0
1000.07	20.8	20.4
1500.23	24.0	23.5

table. In the case of the experimental curves, the amplifier gain was increased by a factor of 20 to define the edge more clearly. The helicon edge depends linearly on the cube root of the frequency as expected.[23]

If a relaxation time of 10^{-9} sec is used, GK oscillations resulting from the large group of electrons with $|\partial A/\partial k_z| = 2.23\times10^8$ cm^{-1} are observed in the calculated curves. These GK oscillations were not observed by Wood and Gavenda[5] but have been observed by others.[18] Due to the cylindrical symmetry employed here no harmonics are observed.

From the slope of a graph of q^2 vs B_0^{-1} the effective number of electrons per unit volume (number of holes per unit volume subtracted from the number of electrons per unit volume) is determined to be 4.9×10^{22} cm^{-3} for both experimental and calculated curves. This value compares with a value 4.3×10^{22} cm^{-3} from magnetoresistance experiments,[24] a value 4.9×10^{22} cm^{-3} from Halse's Fermi-surface parameters, and a value 4.5×10^{22} cm^{-3} from surface-impedance measurements.[25] The value 6.5×10^{22} cm^{-3} reported earlier by Wood and Gavenda[5] was in error.

The value of $|\partial A/\partial k_z|$ associated with those electrons responsible for the helicon edge can be determined from a plot of n^2 (n is the number of half-wavelengths in the sample) vs B_0^{-1}. A maximum or minimum in the transmitted signal occurs when there are an integral number of helicon half-wavelengths in the sample. To determine n for a given magnetic field we assume that there are n_1 half-wavelengths at some arbitrary signal maximum. The adjacent minimum in the transmitted signal occurs when there are $n_1 - 1$ half-wavelengths in the sample (this is the case when the minimum occurs at a higher field than the maximum). If n^2 is plotted as a function of B_0^{-1} a straight line should be obtained for magnetic fields large enough that the local dispersion relation[5] is satisfied. From the local dispersion relation it can also be seen that when $B_0^{-1} = 0$, one obtains $n^2 = 0$. By adjusting the curve so that it passes through the origin, one can read n for any magnetic field directly from the graph. In particular, the value of n at the helicon edge can be determined. The critical factor in the reliability of the determination of $|\partial A/\partial k_z|$ at the helicon edge is that the magnetic fields be high enough for the helicon dispersion relation to be local. The fact that the effective number of electrons per unit volume calculated from the slope of a graph of q^2 vs B_0^{-1} agrees quite well with the value computed from the Halse Fermi surface indicates that the local dispersion relation is satisfied at high fields. A previous conjecture to the contrary by Wood and Gavenda[5] is not correct. The value of $|\partial A/\partial k_z|$ found using $n = 40$ and $B_E = 15.1$ kG (B_E is the value of B_0 at the helicon edge) is 9.5×10^8 cm^{-1}. From Fig. 2 it can be seen that there are sections of the Fermi surface with $|\partial A/\partial k_z| = 9.5\times10^8$ cm^{-1}. Since the effectiveness of a particular band of carriers in damping the helicon via DSCR is proportional[17] to $(\epsilon|\partial^2 A/\partial k_z^2|_{av})^{-1}$, where the subscript av indicates the band-average value, parts of the Fermi surface where $|\partial A/\partial k_z|$ is very steep are not expected to be very effective in damping the helicon. In order to determine the relative damping of the helicon from different bands of electrons and holes, we have calculated the conductivity as a function of q. In Fig. 6, we show Reσ and Imσ as functions of q for a fixed magnetic field of 15.1 kG. For low-q values (or high-B_0 values), there is a sudden increase in Reσ to about one-fourth the value of Imσ. As q is increased, Reσ decreases slightly to about one-fifth Imσ but then begins to increase again until Re$\sigma \approx$ Imσ at high-q values (low-B_0 values). Thus, after the large initial increase in Reσ, Re$\sigma \approx$ Imσ, and the helicon is damped quite effectively.

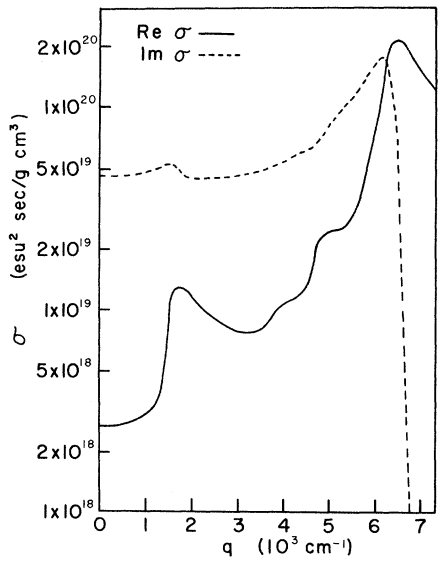

FIG. 6. Real and imaginary parts of σ vs q for $B_0 = 15.1$ kG and $\tau = 10^{-10}$ sec.

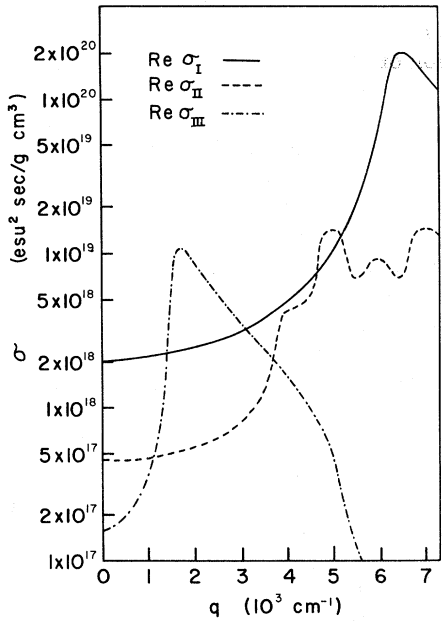

FIG. 7. Real part of σ vs q for each of the three sections as labeled in Fig. 2 for $B_0 = 15.1$ kG and $\tau = 10^{-10}$ sec.

Since conductivities from electron and hole regions are additive and since we wish to determine the contribution to Reσ from carriers on different parts of the Fermi surface, we have also calculated the contribution to Reσ for three sections of the Fermi surface (labeled I, II, and III in Fig. 2). Section I of Fig. 2 consists of electron orbits and extends from $Z = 0$ to $Z = 2.45$. Section II of Fig. 2 consists of four-cornered-rosette hole orbits and extends from $Z = 2.50$ to $Z = 3.80$. Section III of Fig. 2 again consists of electron orbits and extends from $Z = 3.85$ to the limiting point at $Z = 5.20$. From the graph in Fig. 7, we see that the sudden increase in Reσ at low-q values is caused by those electrons in Sec. III of Fig. 2. This does not mean that the contribution to Reσ from Sec. III of Fig. 2 alone will cause the observed helicon edge. The fact that there is contribution to the damping from Sec. I of Fig. 2 should not be surprising since it is well known[13,14,26] that for Fermi surfaces having many electrons associated with a maximum in $|\partial A/\partial k_z|$, the value of q at the helicon edge is much smaller than the q determined from $q(v_z)_{ext} = \omega_c$, where the subscript ext denotes the extremal value.

As q is increased further, the contribution to Reσ from the hole orbits becomes significant while the contribution from Sec. III electrons of Fig. 2 decreases. Finally, at very large-q values the only significant contribution to Reσ comes from Sec. I electrons of Fig. 2. However, since the helicon has been quite effectively damped by other carriers, the pronounced damping effects expected to be produced by the electrons associated with $|\partial A/\partial k_z|_{ext}$ are not seen. The damping effect produced by these electrons has been observed in ultrasonic-attenuation measurements[27,28] and in surface-impedance measurements.[17]

Recent studies[29,30] of GK oscillations at microwave frequencies along the [001] axis in copper report a GK period corresponding to $|\partial A/\partial k_z| = 8.6 \times 10^8$ cm^{-1}. The explanation for this GK period is given in terms of the topological effectiveness of electrons near the necks in region III (polar-orbit region in the nomenclature of Refs. 29 and 30). The origin of this topological effectiveness lies in the reduction of the transverse velocity of an electron as it approaches a neck. It has also been suggested[30] that this topological-effectiveness mechanism may be important in explaining the helicon edges observed by Wood and Gavenda.[5] Since our calculations have been performed assuming a cylindrically symmetric model, the topological-effectiveness concept has not been taken into account. From the agreement of our calculations with experimental results, it would appear that at low frequencies ($\omega \ll \omega_c$), it is sufficient to consider the variation of $A(k_z)$, m_c, and $\partial A/\partial k_z$ with respect to k_z. Other work in aluminum[26] seems to substantiate the fact that the variation of $\partial A/\partial k_z$ is the important point. It is also pointed out[29] that the topological-effectiveness mechanism is not operative whenever $\omega \ll \omega_c$.

B. Results and Interpretation for $\vec{B}_0 \parallel [111]$

In Figs. 8 and 9, we show experimental and calculated curves, respectively, for $\vec{B}_0 \parallel [111]$. In the experimental curve the transmitted signal has been differentiated to enhance the GK oscillations which are superimposed on the slowly varying helicon signal. In each curve the oscillations are periodic in B_0 with a period of 590 ± 7 G. This periodicity

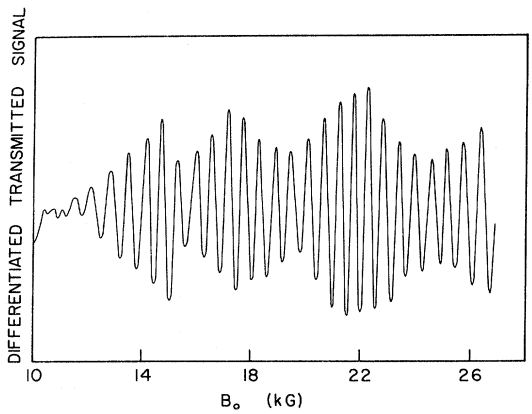

FIG. 8. Differentiated transmitted signal versus B_0 for $\vec{B}_0 \parallel [111]$ with $f = 500.0$ kHz and $L = 0.84$ mm.

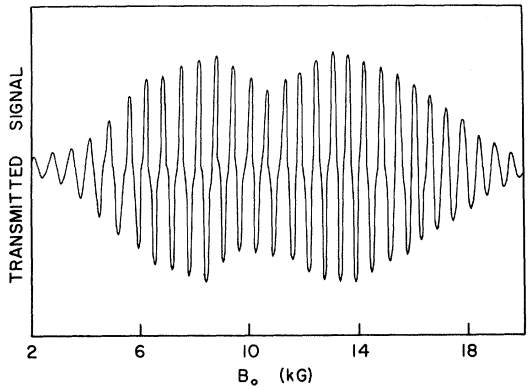

FIG. 9. Calculated transmitted signal versus B_0 for $\vec{B}_0 \parallel [111]$ with $f = 500.0$ kHz and $L = 0.84$ mm and $\tau = 10^{-9}$ sec.

in B_0 is characteristic of GK oscillations. A closer investigation, however, of these curves reveals that their amplitude is modulated. These curves, then, can be interpreted as the beating of two signals whose periods are comparable. In Fig. 4, there are two extremal values of $|\partial A/\partial k_z|$ (one maximum and one minimum) which could give rise to two separate sets of GK oscillations. The modulation period is about 4.5 to 5 kG, but since it is difficult to determine accurately, let us show that the two extremal values of $|\partial A/\partial k_z|$ are consistent with the calculated and experimental results. The expressions which relate the beat period $(\Delta B_0)_b$ and modulation period $(\Delta B_0)_m$ to the periods of the two sets of GK oscillations are given by

$$2/(\Delta B_0)_b = 1/(\Delta B_0)_{\min} + 1/(\Delta B_0)_{\max} \quad (10)$$

and

$$2/(\Delta B_0)_m = 1/(\Delta B_0)_{\min} - 1/(\Delta B_0)_{\max}, \quad (11)$$

where $(\Delta B_0)_{\min}$ and $(\Delta B_0)_{\max}$ denote the periods of the GK oscillations associated with $|\partial A/\partial k_z|_{\min}$ and $|\partial A/\partial k_z|_{\max}$, respectively. If Eq. (9) is inserted into Eqs. (10) and (11) and the values $|\partial A/\partial k_z|_{\max} = 8.05\times10^8$ cm^{-1} and $|\partial A/\partial k_z|_{\min} = 6.50\times10^8$ cm^{-1} are used, the results $(\Delta B_0)_b = 565$ G and $(\Delta B_0)_m = 5.25$ kG are obtained. These values for $(\Delta B_0)_b$ and $(\Delta B_0)_m$ are consistent with the observed values in both the calculated and experimental results.

V. SUMMARY

Helicon propagation and GK oscillations have been investigated numerically in copper. Good agreement between calculated curves and experimental curves was obtained using only the correct variation of $A(k_z)$, $\partial A/\partial k_z$, and m_c. For $\vec{B}_0 \parallel [001]$, the relative damping effects of carriers on different parts of the Fermi surface were discussed. For $\vec{B} \parallel [111]$, modulated GK oscillations were observed and interpreted as the beating of two sets of GK oscillations.

ACKNOWLEDGMENTS

We wish to express our appreciation to Dr. J. B. Coon and Dr. T. W. Johnston for valuable discussions. We also thank the University of Houston Computing Center for making its facilities available.

*Supported in part by the University of Houston Faculty Research Support Program.

[1]P. M. Platzman and S. J. Buchsbaum, Phys. Rev. 132, 2 (1963).

[2]G. A. Baraff, Phys. Rev. 167, 625 (1968).

[3]P. R. Antoniewicz, Phys. Rev. 185, 863 (1969).

[4]P. R. Antoniewicz, L. T. Wood, and J. D. Gavenda, Phys. Rev. Letters 21, 998 (1968).

[5]L. T. Wood and J. D. Gavenda, Phys. Rev. B 2, 1492 (1970).

[6]P. Aigrain, in *Proceedings of the International Conference on Semiconductor Physics, Prague*, 1960 (Czechoslovak Academy of Science, Prague, 1961), p. 224.

[7]O. V. Konstantinov and V. I. Perel, Zh. Eksperim. i Teor. Fiz. 38, 161 (1960) [Sov. Phys. JETP 11, 117 (1960)].

[8]R. Bowers, C. Legendy, and F. E. Rose, Phys. Rev. Letters 7, 339 (1961).

[9]For a more complete list of references see the review article by B. W. Maxfield, Am. J. Phys. 37, 241 (1969).

[10]V. F. Gantmakher and E. A. Kaner, Zh. Eksperim. i Teor. Fiz. 48, 1572 (1965) [Sov. Phys. JETP 21, 1053 (1965)].

[11]J. Mertsching, Phys. Status Solidi 26, 9 (1968).

[12]A. W. Overhauser and S. Rodriguez, Phys. Rev. 141, 431 (1966).

[13]J. C. McGroddy, J. L. Stanford, and E. A. Stern, Phys. Rev. 141, 437 (1966).

[14]D. S. Falk, B. Gerson, and J. F. Carolan, Phys. Rev. B 1, 406 (1970).

[15]E. A. Stern, Phys. Rev. Letters 10, 91 (1963).

[16]G. Weisbuch and A. Libchaber, Phys. Rev. Letters 19, 498 (1967).

[17]S. W. Hui, Phys. Rev. 185, 988 (1969).

[18]B. Perrin, G. Weisbuch, and A. Libchaber, Phys. Rev. B 1, 1501 (1970).

[19]M. R. Halse, Phil. Trans. Roy. Soc. London A265, 507 (1969).

[20]P. B. Miller and R. R. Haering, Phys. Rev. 128, 126 (1962).

[21]J. F. Koch, R. A. Stradling, and A. F. Kip, Phys. Rev. 133, A240 (1964).

[22]P. T. Coleridge and B. R. Watts, Can. J. Phys. 49, 2379 (1971).

[23]J. L. Stanford and E. A. Stern, Phys. Rev. 144, 534 (1966).

[24]J. R. Klauder, W. A. Reed, G. F. Brennert, and J. E. Kunzler, Phys. Rev. 141, 592 (1966).

[25]S. W. Hui, J. Appl. Phys. 40, 3521 (1969).

[26]P. K. Larsen and F. C. Greisen, Phys. Status Solidi 45, 363 (1971).

[27]J. R. Boyd and J. D. Gavenda, Phys. Rev. 152, 645 (1966).

[28]M. H. Jericho and A. M. Simpson, Phil. Mag. 17, 267 (1968).
[29]G. A. Baraff and T. G. Phillips, Phys. Rev. Letters 24, 1428 (1970).
[30]T. G. Phillips, G. A. Baraff, and P. H. Schmidt, Phys. Rev. B 5, 1283 (1972).

PHYSICAL REVIEW B VOLUME 6, NUMBER 4 15 AUGUST 1972

Energy Dependence of the Effective Debye Temperature Obtained from Low-Energy–Electron-Diffraction-Intensity Measurements*

G. E. Laramore
Sandia Laboratories, Albuquerque, New Mexico 87115
(Received 11 February 1972)

A discussion of the effect of lattice vibrations on the effective electron–ion-core elastic scattering vertex is given using the model of Duke and Laramore. The renormalization introduced by the lattice vibrations can substantially increase the number of partial waves necessary to describe this scattering. The vertex approximation using the s-wave part of the phonon renormalization factor and phase shifts from a realistic potential to describe the electron–rigid-ion scattering is compared with the vertex approximation using the full phonon renormalization factor and the constant phase shift s-wave model to describe the electron–rigid-ion scattering. Model calculations of low-energy–electron-diffraction (LEED) intensity profiles are presented for a system having the geometrical parameters of Al(100), and effective Debye temperatures are obtained for the Bragg peaks in the intensity profiles. The dependence of these effective Debye temperatures on the ineleastic-collision mean free path and on the characteristic falloff of the vibrational amplitude of the ion cores with distance from the surface is investigated. Even for a constant mean free path the Θ_D^{eff} exhibit a pronounced energy dependence. By comparing the calculated Θ_D^{eff} with the experimental measurements of Quinto *et al.*, a crude estimate of the inelastic-collision mean free path in the surface region of aluminum is obtained.

I. INTRODUCTION

It is well known that lattice vibrations introduce a temperature dependence into the intensities of x rays[1] and neutrons[2] scattered by a solid. Since the x rays and neutrons interact only weakly with the ion cores of the solid, their scattering can be treated in linear response theory and so the temperature dependence of the scattered beams can be simply related to a Debye temperature[3] which characterizes the vibrational amplitudes of the ion cores in the "bulk" region of the solid. Low-energy electrons, on the other hand, interact quite strongly with the ion cores of the solid and also with the high-energy electronic excitations (e.g., plasmons, interband transitions). These effects greatly complicate the interpretation of the temperature dependence of the elastic scattering intensity for electrons.[4,5] However, it is an experimental fact that the temperature dependence of the intensity of maxima in low-energy–electron-diffraction (LEED) intensity profiles can be described in terms of an effective Debye temperature.[6–15] A common feature of these observations is that in a given intensity profile the low-energy maxima are characterized by a smaller effective Debye temperature Θ_D^{eff} than the higher-energy maxima. This smaller Θ_D^{eff} for the lower-energy peaks is indicative of a larger amplitude of vibration for the surface atoms than for those atoms in the "bulk" region of the solid. Duke and Laramore[4,5] investigated the consequences of lattice vibrations in a theoretical calculation of the LEED intensity profiles and showed that for the range of electron energies commonly used in LEED, their main effect was to renormalize the effective electron–ion-core elastic scattering vertex, making it temperature dependent. They investigated the effects of a vibronically inequivalent surface layer[5] on the temperature dependence of the elastic intensity profiles and showed that although the temperature dependence of the peaks in the intensity profiles could be described in terms of a Θ_D^{eff}, this effective Debye temperature could not be simply related to the vibrational amplitudes of either the surface or the bulk ion cores. The Θ_D^{eff} obtained from this analysis depends as well on the relative scattering strengths of the surface and bulk ion cores and upon the inelastic mean free path which determines the relative sampling of the surface and bulk regions of the elastic beam.

Recent model calculations[16–22] indicate that for a clean surface it is reasonable to use the same potential to describe the interaction between the beam electrons and both the surface and bulk ion cores of the solid. The rationale for this is that the electron